A DECREASE IN CELLULAR ENERGY STATUS STIMULATES PERK-DEPENDENT eIF2α PHOSPHORYLATION AND REGULATES PROTEIN SYNTHESIS IN PANCREATIC β-CELLS.

Edith Gomez*§, Mike L. Powell*§, Alan Bevington¶ and Terence P. Herbert*‡
From the Departments of Cell Physiology and Pharmacology* and Infection, Immunity & Inflammation¶, Faculty of Medicine and Biological Sciences, The Henry Wellcome Building, University of Leicester, University Road, Leicester LE1 9HN, United Kingdom.

Running title: PERK, an intracellular energy sensor

§EG and MLP contributed equally to this work

‡Address correspondence to: Dr. T. P. Herbert, The Department of Cell Physiology and Pharmacology, Faculty of Medicine and Biological Sciences, The Henry Wellcome Building, University of Leicester, University Road, Leicester LE1 9HN, United Kingdom.
Tel: +44 (0)116 229 7148, e-mail: tph4@le.ac.uk

Key words: Translation, eIF2α, PERK, β-cell, energy status, glucose

Acknowledgements.

This work was supported by a Wellcome Trust Project Grant (awarded to TPH). EG was supported by the Wellcome Trust. MLP was supported by an MRC studentship. We would also like to thank Professors Ron Wek, David Ron and Chris Proud for generously providing reagents.

Abbreviations.

MIN6, mouse insulinoma cell line 6; ER, Endoplasmic Reticulum; PAGE, polyacrylamide gel electrophoresis; KRB, Krebs-Ringer bicarbonate buffer; eIF2, eukaryotic initiation factor 2; PERK, PKR-like Endoplasmic Reticulum Kinase; UPR, unfolded protein response; IRE1, inositol requiring enzyme 1; BiP, Immunoglobulin binding protein; AMPK, AMP activated protein kinase; VGCC, voltage gated calcium channels.

In this report we demonstrate that, in pancreatic β-cells, eIF2α phosphorylation in response to a decrease in glucose concentration is primarily mediated by the activation of PKR-like ER kinase (PERK). We provide evidence that this increase in PERK activity is evoked by a decrease in the energy status of the cell via a potentially novel mechanism that is independent of IRE1 activation and the accumulation of unfolded nascent proteins within the ER. The inhibition of eIF2α phosphorylation in glucose deprived cells by the over-expression of dominant-negative PERK or an N-terminal truncation mutant of GADD34 leads to a 53% increase in the rate of total protein synthesis. Polysome analysis revealed that this coincides with an increase in the amplitude but not the number of ribosomes per mRNA, indicating that eIF2α dephosphorylation mobilises hitherto untranslated mRNAs onto polysomes. In summary, we show that PERK is activated at low glucose in response to a decrease in energy status and that this plays an important role in glucose regulated protein synthesis in pancreatic β-cells.

Introduction.

Glucose stimulated insulin secretion from pancreatic β-cells is mediated by a series of steps initiated by the metabolism of glucose, which results in an increase in the cellular ATP/ADP ratio. This increase in the ATP/ADP ratio causes the closure of ATP sensitive potassium channels, leading to membrane depolarisation and the subsequent opening of L-type voltage gated calcium channels (VGCC). The resultant influx of calcium activates the exocytotic machinery, resulting in the secretion of insulin (for review see [1]). Glucose also stimulates a rapid increase in the rate of proinsulin synthesis (up to 20-fold within 1h), the co-ordinate increase in the rate of synthesis of a large subset of proteins and a two-fold increase in the rate of total protein synthesis [2-11]. These acute changes in the rate of protein synthesis are almost entirely regulated at the post-transcriptional level [2-11] and, like insulin secretion, require the metabolism of glucose [12]. However, the metabolic signals emanating from the mitochondrial metabolism of glucose that stimulate secretion are distinct from those that stimulate protein synthesis [12, 13].

An important rate limiting step in protein synthesis is the assembly of the translational ternary complex, made up of the methionyl initiator tRNA (Met-tRNA$_i$) attached to eukaryotic initiation factor 2 (eIF2) in its GTP bound state (eIF2-GTP:Met-tRNA$_i$) (for review see [14]). This ternary complex binds to the 40S ribosomal subunit which, in association with additional initiation factors, delivers the Met-tRNA$_i$ to the mRNA translational start site. Following translational start site recognition, the GTP bound to eIF2 is hydrolysed to GDP, rendering eIF2α unable to bind initiator methionyl tRNA. Therefore, in order to take part in further rounds of initiation, eIF2-GDP must be recycled back to eIF2-GTP. The 'recycling' of

eIF2-GDP to eIF2-GTP is catalysed by the guanine nucleotide exchange factor (GEF) eIF2B. Since active eIF2-GTP is required for the recruitment of Met-tRNA$_i$, changes in the activity of eIF2B are important in regulating the rate of translation initiation [15]. eIF2B activity is regulated by a number of mechanisms including phosphorylation of its ε-subunit by GSK3 [16, 17], allosteric regulation [18, 19], and competitive inhibition by phosphorylation of the alpha subunit of its substrate eIF2 (eIF2α) on Serine 51 [20, 21]. Competitive inhibition of eIF2B by phosphorylated eIF2α is the most studied and best characterised mechanism by which eIF2B activity is regulated.

eIF2α phosphorylation occurs in response to a wide array of cellular stresses mediated by one of four eIF2α kinases: the double stranded RNA-dependent eIF2α kinase (PKR), the mammalian orthologue of the yeast GCN2 protein kinase (mGCN2), the heme-regulated eIF2α kinase (HRI) and the PKR-like endoplasmic reticulum kinase (PERK). PKR expression is induced by interferon and is activated in response to dsRNA [22, 23]. In yeast, GCN2 phosphorylates eIF2α in response to uncharged tRNAs (amino acid deprivation) and glucose starvation [14, 24, 25]. However, the role of the mammalian orthologue (mGCN2) is less clear. HRI is activated in response to heme-deprivation in erythroid cells [26] and PERK is activated in response to protein malfolding in the endoplasmic reticulum (ER) as part of the unfolded protein response (UPR) [27-29]. It has been speculated that the UPR may be activated in response to high glucose concentration due to increased rates of protein synthesis exceeding the folding capacity of the ER and resulting in the accumulation of unfolded proteins and the activation of PERK [27, 30-32].

We have previously demonstrated, in islets of Langerhans and in the pancreatic β-cell line MIN6, that the availability of the translational ternary complex is increased in response to glucose [11] and that this was likely mediated through the dephosphorylation of eIF2α. In MIN6 cells, changes in both the availability of ternary complex and the phosphorylation status of eIF2α paralleled changes in protein synthesis, leading us to hypothesise that eIF2α phosphorylation is likely to play a key role in glucose stimulated protein synthesis [11]. Moreover, in MIN6 cells, increases in eIF2α phosphorylation in response to a temporally acute decrease in glucose concentration parallel the recruitment of mRNAs encoding integrated stress response genes onto polysomes [33]. Recently, it has been reported that, in MIN6 cells, eIF2α dephosphorylation in response to increasing glucose concentrations is mediated, at least in part, by an increase in PP1 activity towards eIF2α [34]. However, the eIF2α kinase that phosphorylates eIF2α at low glucose concentration in pancreatic β-cells and its role in glucose regulated protein synthesis is unknown.

Materials and Methods.

Chemicals and Materials. DMEM was obtained from Sigma. Foetal calf serum was purchased from Invitrogen. [^{35}S]-methionine was obtained from MP Biomedicals UK. All other chemicals were purchased from Sigma unless otherwise stated.

Cell Culture and Treatment. In this study, MIN6 cells (kindly provided by Prof. Jun-Ichi Miyazaki) were used between passages 25-40 at ~80% confluence. MIN6 cells were grown in DMEM containing 25mM glucose supplemented with 15% heat-inactivated foetal calf serum, 100μg/ml streptomycin, 100 units/ml penicillin sulfate, 75μM β-mercaptoethanol and 40mM sodium bicarbonate, equilibrated with 5% CO_2, 95% air at 37°C. Prior to treatment, the medium was removed and the cells were washed twice with Krebs-Ringer bicarbonate buffer (KRB) (115mM NaCl, 5mM KCl, 10mM $NaHCO_3$, 2.5mM $MgCl_2$, 2.5mM $CaCl_2$, 20mM HEPES pH 7.4 supplemented with 0.5% bovine serum albumin (BSA)). The cells were then incubated for 1h at 37°C in KRB (unless otherwise stated) prior to incubation in KRB or KRB containing 20mM glucose for a further hour at 37°C (unless otherwise stated). Full details of treatments are provided in the figure legends. After treatment, the cells were washed with ice cold PBS and then lysed by the addition of ice-cold lysis buffer containing 1% triton, 10mM β-glycerophosphate, 50mM tris-HCl pH 7.5, 1mM EDTA, 1mM EGTA, 1mM sodium orthovanadate, 1mM benzamidine-HCl, 0.2mM phenylmethylsulfonyl fluoride, 1 μg/ml each of leupeptin and pepstatin, 0.1% β-mercaptoethanol and 50mM sodium fluoride (unless otherwise stated). The lysates were then centrifuged for 10min at 16000 g. The supernatants were kept and total protein concentrations were determined by the Bradford assay (Bio-Rad) using BSA as standard. The protein lysates were stored at –80°C until further analysis.

Determination of Cellular ATP content. ATP content was determined using a bioluminescent assay (Sigma) following the manufacturer's instructions. Briefly, following treatments, as described above and in the figure legends, cells were lysed by the addition of somatic cell ATP releasing reagent. Luminescence was then read immediately in a Novostar (BMG Labtech) 96 well plate reader with injectors.

Adenoviral construction and Infection. Recombinant adenoviruses expressing amino acids 1-583 of PERK (i.e. dominant negative PERK (Ad-PERKΔC)) and GFP (Ad-empty) have been previously described [11]. In order to generate pAdTrack-GADDΔN, GADD34 cDNA was amplified by PCR from a mouse cDNA library generated from MIN6 cells using the primers GADD34-N-F721 5' AGC GAA TTC TCT AGA GAG AAG CCT AAG 3' and GADD34R-UTR 5' TAT CTC GAG GGA AAC TAC TCA GGC TTA GCC 3'. The resultant cDNA was digested with *EcoRI* and *XhoI* and subcloned into *EcoRI* and *XhoI* digested pCMV-

Tag3b creating pCMV-Tag-GADDΔN, encoding the C-terminal end of GADD34 fused in frame with an N-terminal myc epitope tag. Myc-tagged GADDΔN was amplified by PCR using primers GADD34-FMYC 5'AGC GGT ACC ATG GAG CAG AAA CTC ATC 3' and GADD34R-3UTR 5'TAT CTC GAG GGA AAC TAC TCA GGC TTA GCC 3'. The PCR product was digested with *KpnI* and *XhoI* and subcloned into *KpnI* and *XhoI* digested pAdTrack-CMV. The resulting plasmid pAd-GADDΔN was used to generate the recombinant adenovirus Ad-GADDΔN as previously described [11]. For infection, MIN6 cells were incubated in the presence of the virus for 48h prior to treatments [11]. Under these conditions, >90% of cells were infected, as determined by EGFP expression using fluorescence microscopy.

Silencing of PERK Expression Using Small Interfering RNAs. PERK expression was specifically silenced in MIN6 cells using 25 nucleotide prevalidated siRNA duplexes (Stealth ™ Select RNAi) purchased from Invitrogen directed against mouse PERK (siRNA20-Sense 5'UAGAGGAGUUCAAACAGAAUCAAGC3'- antisense 5'CGUUGAUUCUGUUUGAACUCCUCUA3' and siRNA21-Sense 5'UCUUUGAACCAUCAUAUGCUCUUGGG 3'- antisense 5'CCCAAGAGCAUAUGAUGGUUCAAGA3'). An siRNA, which showed no significant homology to any known protein was used as a control (Con siRNA- Sense 5'CGUGAUUGCGAGACUCUGATT3'- antisense 5'UCAGAGUCUCGCAAUCACGTT 3'). SiRNAs were introduced into MIN6 cells by electroporation using a pipette-type electroporator (Microporator MP-100 from Digital Bio). Transfections were performed according to the manufacturer's instructions. Typically, transfection >90% were obtained as assessed by monitoring the transfection efficiency of a fluorescent siRNA (Block-it™ fluorescent oligo from Invitrogen).

Protein Synthesis Measurements. Protein synthesis measurements were performed essentially as described previously [35]. Briefly, cells were incubated in the presence of [^{35}S]-methionine for the times indicated in the text. Cell lysates (as described in *Cell Culture and Treatment*) were prepared and equal amounts of protein (about 20μg) were spotted onto 3MM Whatmann filters. The filters were then washed by boiling them for 1 min in 5% trichloroacetic acid containing 0.1g/litre of methionine. This was repeated three times. The filters were then dried and immersed in scintillant before determining radioactivity by scintillation counting.

SDS-PAGE and Western Blotting. SDS-PAGE and Western blotting were performed as described previously [35]. Anti-phospho eIF2α (Ser-51) antibody was purchased from Biosource. Anti-phospho AMP-activated kinase

(AMPK) (Thr-172) was purchased from Cell Signalling Technologies, MA, USA. Anti-IRE1 and anti-phospho IRE1 (Ser724) were purchased from Novus Biologicals Inc, CO, USA. Anti-PERK antibody was kindly provided by Prof. Ronald Wek (Indiana University School of Medicine, USA) and anti-eIF2α antibody was a generous gift from Prof. Chris Proud (Columbia University, Vancouver, Canada)

PCR-Based Assay for XBP-1 Splicing. After treatments, as described in the figure legend, total RNA was prepared from cells using TRI reagent (Sigma) and first-strand cDNA were synthesized from 4 μg of each sample using SuperScript^{TM}II Reverse Transcriptase (Invitrogen) according to the manufacturer's instructions. xbp-1 processing is characterised by excision of a 26bp sequence from the coding region of xbp-1 mRNA [36]. Thus the cDNA prepared were used as template for PCR using primers flanking the splice site, as described by Marciniak et al. [37]. Unspliced xbp-1 gave a product of 480bp, and the spliced cDNA was 454bp. The cleaved 26bp fragment contains a Pst1 restriction site, and so the extent of xbp-1 processing can be evaluated by restriction analysis [38]. PCR products were purified and digested with Pst1 restriction enzyme. Restriction digests were separated on 3% agarose gel containing ethidium bromide. PCR products derived from unspliced xbp-1 mRNA (indicating absence of ER stress) were digested in two bands of 290bp and 190bp. In contrast, products amplified from spliced xbp-1 mRNA were resistant to digestion and remained 454bp long, indicating presence of ER stress.

*Polysome profile Analysis***.** After treatment, cells were lysed in polysome buffer (20mM HEPES pH 7.6, 15mM $MgCl_2$, 300mM KCl, 1 mg/ml heparin, 0.1mg/ml cycloheximide, 1 mM DTT, 1μl/ml RNAguard^{TM}, 1mM benzamidine-HCl, 0.1mM phenylmethylsulfonyl fluoride, 1 μg/ml leupeptin and 1 μg/ml pepstatin) supplemented with 1% triton. Cell lysates were centrifuged for 10 min at 13000g at 4°C to remove nuclei and cell debris. The supernatants were then layered onto 20-50% sucrose gradients (made in polysome buffer) and centrifuged at 39000rpm for 2h at 4°C in a Sorvall TH64.1 rotor. The gradients were fractionated using an ISCO gradient fractionator that continuously measured absorbance at 254nm.

Results

PERK is activated upon glucose deprivation. To investigate whether the eIF2α kinase PERK is activated by glucose deprivation, MIN6 cells were mock infected or infected with a recombinant adenovirus over-expressing a dominant-negative mutant of PERK (AdPERKΔC). 48h post-infection, the cells were incubated in KRB without glucose or containing 20mM glucose in the presence or absence of thapsigargin (an ER stress inducing agent known to lead to the activation of PERK) as a positive control. The activation of PERK was assessed by

its migration on SDS-PAGE using antisera against total PERK (Fig. 1a). In the mock infected cells, glucose deprivation and thapsigargin treatment resulted in a decrease in PERK mobility on SDS-PAGE, consistent with PERK phosphorylation, and an increase in the phosphorylation of its substrate eIF2α (Fig. 1a). The over-expression of PERKΔC inhibited PERK's mobility shift and eIF2α phosphorylation induced in response to glucose deprivation and thapsigargin. These results demonstrate that PERK is activated upon glucose deprivation and that PERK activation is primarily responsible for eIF2α phosphorylation in glucose deprived cells. To provide additional evidence that PERK is responsible for the phosphorylation of eIF2α in response to glucose deprivation, the expression of PERK was knocked-down in MIN6 cells using two distinct sets of siRNAs. The expression of PERK was reduced by up to 80% which resulted in a 41-45% and a 34-41% reduction in eIF2α phosphorylation in response to either glucose deprivation or thapsigargin treatment respectively (Fig. 1b). Taken together these results provide good evidence that PERK phosphorylates eIF2α in glucose deprived MIN6 cells.

To determine whether these PERK-dependent increases in eIF2α phosphorylation in response to glucose deprivation also occur at physiologically relevant glucose concentrations, MIN6 cells were mock infected or infected with the recombinant adenovirus AdPERKΔC and incubated in KRB containing 0, 2, 5, 7.8, 10, 20 or 40mM glucose and, as a positive control, thapsigargin (Fig. 1c). In mock infected cells, the phosphorylation of eIF2α increased with decreasing glucose concentrations. Importantly, the expression of PERKΔC inhibited the phosphorylation of eIF2α (Fig. 1c) at all glucose concentrations tested. This provides evidence that PERK is activated in response to physiologically relevant decreases in glucose concentrations.

We had previously reported that PERK was unlikely to be responsible for the phosphorylation of eIF2α at low glucose concentration [11]. This conclusion was primarily based on results showing that, at low glucose concentration, PERK was not significantly phosphorylated at Thr980. However, it is likely that the anti-phospho PERK Thr980 antibody used in our previous study was not sensitive enough to consistently detect changes in PERK phosphorylation at low glucose concentrations.

Decreases in Intracellular Energy Status activate PERK. Given that protein folding is an energy dependent process, one possible effector of PERK activation is a fall in the energy status of the cell in response to a decrease in glucose concentration. To investigate this possibility, we initially determined whether mitochondrial inhibitors of the electron transport chain could activate PERK and stimulate the phosphorylation of eIF2α (Fig. 2). Treatment of

MIN6 with three distinct mitochondrial inhibitors of the electron transport chain (Rotenone, an inhibitor of complex I; sodium azide, an inhibitor of complex IV; and oligomycin, which blocks the F_0 proton channel of ATP synthase) all led to the phosphorylation of PERK and the phosphorylation of eIF2α (Fig. 2a). All inhibitors had similar effects on intracellular ATP content, reducing ATP to less than 1/6 of that of the control (Fig. 2b). Therefore, a decrease in the energy status of MIN6 cells can stimulate the activation of PERK and the phosphorylation of eIF2α. To investigate whether physiological decreases in energy status also lead to the activation of PERK and eIF2α phosphorylation, we artificially reduced cellular ATP content and the energy status of the cell to within the range observed in glucose deprived cells using oligomycin (Fig. 3). Increasing oligomycin concentrations led to a dose-dependent decrease in intracellular ATP content (Fig. 3a) and the energy status of the cell, as assessed by the phosphorylation state of AMP-activated protein kinase (AMPK) (a sensor of intracellular AMP and hence cellular energy status [39]) (Fig. 3b). Importantly, oligomycin induced decreases in cellular energy status that were within the range seen in glucose deprived cells caused similar increases in eIF2α phosphorylation, which paralleled increases in the phosphorylation of PERK (Fig. 3b and c). Increasing oligomycin concentrations also led to a dose-dependent decrease in the rate of [^{35}S]-methionine incorporation into protein, relative to the cells incubated at 20mM glucose alone (Fig 3d). Interestingly, decreases in energy status/ATP alone are not solely responsible for the dramatic decrease in the rate of protein synthesis observed in glucose deprived cells as oligomycin induced decreases in ATP/energy status similar to that evoked by glucose deprivation led to a comparatively small decrease in the rate of protein synthesis compared to that evoked by glucose deprivation (Fig. 3).

To confirm that oligomycin stimulated eIF2α phosphorylation by activating PERK, MIN6 cells were mock infected or infected with a recombinant adenovirus over-expressing a dominant-negative mutant of PERK (AdPERKΔC). 48h post-infection, the cells were incubated in KRB or KRB plus 20mM glucose in the presence or absence of increasing concentrations of oligomycin (Fig. 3e). In the mock infected cells, increasing concentrations of oligomycin led to a dose-dependent decrease in the mobility of PERK on a SDS-polyacrylamide gel, consistent with PERK phosphorylation. This phosphorylation of PERK paralleled increases in the phosphorylation of eIF2α (Fig. 3e). Over-expression of PERKΔC resulted in an inhibition of PERK's phosphorylation in response to all doses of oligomycin tested and in response to glucose deprivation. These decreases in PERK phosphorylation correlated with a decrease in eIF2α phosphorylation (Fig. 3e), demonstrating that oligomycin evokes the phosphorylation of eIF2α via the activation of PERK.

AMPK Activation does not stimulate eIF2α Phosphorylation or Protein Synthesis in Pancreatic β-cells. As the activation of AMPK parallels eIF2α phosphorylation (see Fig. 3), we investigated whether AMPK plays a role in the regulation of eIF2α phosphorylation or indeed glucose regulated protein synthesis. MIN6 cells were pre-incubated for 1h in KRB at 0mM glucose before treatment for a further hour at either 0mM or 20mM glucose, or 20mM glucose in the presence of increasing concentrations of 5'-phosphoribosyl-5-aminoimidazole-4 carboxamide (AICAR), a pharmacological activator of AMPK (Fig. 4a). As expected, glucose deprivation led to a significant increase in the phosphorylation of eIF2α (Fig. 4a) that correlated with an increase in AMPK activation, as assessed using a phospho-specific antibody to Thr172 of AMPK. However, when cells were treated with increasing concentrations of AICAR, AMPK phosphorylation was not accompanied by an increase in eIF2α phosphorylation (Fig. 4a). Additionally, AICAR had no inhibitory effect on glucose-stimulated protein synthesis (Fig. 4b). These data provides evidence that neither changes in eIF2α phosphorylation nor protein synthesis are mediated via changes in the activity of AMPK.

Investigation into the Mechanism of PERK Activation in Response to Glucose Deprivation. Transducers of the unfolded protein response (UPR) include two related ER transmembrane serine-threonine kinases, PERK and inositol requiring enzyme-1 (IRE1) (an RNAse required for the splicing and activation of the X-box transcription factor XBP1). PERK and IRE1 are thought to be activated by a similar mechanism requiring homo-oligomerisation, possibly initiated by the dissociation of BiP from their ER luminal domains [28, 40, 41]. As glucose deprivation leads to the activation of PERK, we investigated whether glucose deprivation also resulted in the activation of IRE1 (Fig 5a). Initially, we investigated the auto-phosphorylation state of IRE1 on Ser724, whose phosphorylation is required for IRE1 activation (Fig 5ai). MIN6 cells were incubated in KRB or DMEM containing 0 or 20mM glucose or treated with thapsigargin as control (Fig 5ai). IRE1 was more phosphorylated on Ser724 in MIN6 cells incubated at 20mM glucose compared to that seen in glucose deprived cells, indicating that IRE1 was possibly inactivated in glucose deprived cells. To assay IRE1 activity, IRE1-dependent splicing of its substrate, the XBP1 mRNA was determined by RT-PCR (Fig. 5aii). In this case, MIN6 cells were maintained in complete media or incubated in either KRB (0mM glucose), KRB supplemented with 0.5mM glucose or KRB supplemented with 20mM glucose for 2, 16 and 24h. As a positive control, cells were also treated with thapsigargin for 2 or 4h. As anticipated, treating cells with thapsigargin led to a large increase in the spliced form of the XBP1 mRNA (Fig. 5aii). The transfer of cells from full media (c) containing

25mM glucose to KRB or KRB supplemented with 0.5mM or 20mM glucose led to a decrease in the amount of the spliced form of XBP1 (Fig. 5aii). However, in cells incubated in KRB supplemented with 20mM glucose for 16h and 24h an increase in the spliced form of XBP1 was observed. Therefore, IRE1 is inactive in glucose deprived cells or cells incubated at low glucose concentrations, whereas IRE1 is activated at high glucose concentrations. These results are in agreement with previous reports investigating IRE1 activation in response to differing glucose concentrations in Islets [32]. As IRE1 is not activated by glucose deprivation and PERK is, the mechanism or threshold of activation of PERK must differ from that of IRE1.

PERK and IRE1 are classically activated by the accumulation of unfolded proteins within the ER, where ER client load exceeds the folding capacity of the ER. Therefore, to investigate whether the accumulation of nascent unfolded/incompletely processed proteins within the ER led to PERK activation under conditions of glucose deprivation, MIN6 cells were incubated in the presence of cycloheximide for 1h (preinc) to inhibit protein synthesis and allow nascent proteins undergoing processing within the ER to be chased into mature processed proteins (Fig. 5b). The cells were then further incubated in the presence of cycloheximide for an hour in the absence or presence of 20mM glucose and the levels of eIF2α phosphorylation compared to cells in which cycloheximide had not been added. To ascertain whether nascent proteins within the ER were fully processed during the 1h preincubation with cycloheximide and that cycloheximide had effectively blocked further protein synthesis, [^{35}S]-methionine was added to the cells 15min prior to the preincubation (P) and left on the cells during the preincubation period. The incorporation of [^{35}S]-methionine into proinsulin, insulin and total protein was assessed by SDS-PAGE (Fig. 5bi). In the presence of cycloheximide, no increase in protein synthesis was detected (compare lanes 1 to 3). Additionally, the labelled proinsulin was no longer detectable after 1h incubation with cycloheximide (compare lanes 1 to 3), indicating that the proinsulin had been fully processed to insulin and presumably chased out of the ER/cell (Fig. 5bi). At high glucose concentration, cycloheximide reduced eIF2α phosphorylation (Fig. 5bii), indicating that ER client load and the accumulation of unfolded proteins may contribute to ER stress and the activation of PERK as previously predicted [32]. In contrast, in the absence of glucose, cycloheximide treatment had no significant effect on eIF2α phosphorylation (Fig. 5bii). This indicates that the accumulation of unfolded/unprocessed nascent proteins is unlikely to account for the activation of PERK under conditions of glucose deprivation.

PERK Dependent eIF2α Phosphorylation Contributes to the Suppression of Protein Synthesis at Low Glucose. To investigate the role of PERK-dependent eIF2α phosphorylation in

the suppression of protein synthesis and proinsulin synthesis at low glucose, MIN6 cells were infected with an empty adenovirus (Ad-Empty), a recombinant adenovirus expressing a dominant-negative mutant of PERK (AdPERKΔC) or an N-terminal truncation mutant of GADD34 (AdGADDΔN) which constitutively directs protein phosphatase-1 to eIF2α leading to eIF2α dephosphorylation. 48h post-infection, the cells were incubated in KRB without glucose or containing 20mM glucose in the presence or absence of thapsigargin as a positive control. The phosphorylation state of PERK and eIF2α were assessed by Western blotting (Fig. 6ai). In the control cells infected with Ad-Empty, glucose deprivation and thapsigargin treatment resulted in a decrease in PERK mobility on SDS-PAGE, consistent with PERK phosphorylation. This phosphorylation of PERK by either glucose deprivation or thapsigargin paralleled increases in the phosphorylation of eIF2α and decreases in the rate of protein synthesis compared to cells incubated in 20mM glucose (Fig. 6ai and ii). Over-expression of PERKΔC or GADDΔN significantly inhibited eIF2α phosphorylation induced in response to glucose deprivation and thapsigargin treatment (Fig. 6ai) and, as expected, significantly overcame the inhibition of protein synthesis induced by thapsigargin (Fig. 6aii). Importantly, over-expression of PERKΔC or GADDΔN increased protein synthesis by a mean average of 53% in glucose deprived cells but still only partially overcame the inhibitory effects of glucose deprivation on protein synthesis. The over-expression of PERKΔC or GADDΔN had similar effects on the synthesis of proinsulin, indicating that eIF2α phosphorylation does not play a specific role in glucose regulated proinsulin synthesis (Fig 6aiii). Analysis of the polysome profiles from glucose deprived MIN6 cells over-expressing PERKΔC or GADDΔN demonstrate that the inhibition of eIF2α phosphorylation leads to an increase in the amplitude of the polysomes but not in the number of ribosome loaded onto mRNA (Fig. 6b). One possible explanation is that the inhibition of eIF2α phosphorylation in glucose deprived cells stimulates the recruitment of otherwise dormant mRNAs into polysomes.

Discussion

In this report we present evidence that PERK is activated in pancreatic β-cells in response to a decrease in glucose concentration. This increase in PERK activity is evoked by a decrease in the energy status of the cell through a potentially novel mechanism, independent of the accumulation of nascent unfolded proteins within the ER and the activation of IRE1. We also demonstrate that the phosphorylation of eIF2α at low glucose plays an important role in suppressing global rates of protein synthesis in pancreatic β-cells.

The mechanism by which PERK is activated by decreased glucose concentration/energy status is unknown. Yet, it has previously been hypothesised that glucose starvation may,

through a decrease in UDP-NAcHexosamines production, inhibit protein glycosylation, resulting in the accumulation of unprocessed proteins within the ER and the activation of PERK [42]. Indeed, in a number of cell types, tunicamycin, an inhibitor of glycosylation, activates PERK and the UPR [27]. However, the mitochondrial metabolism of pyruvate is sufficient to stimulate the dephosphorylation of eIF2α in glucose deprived MIN6 cells, via a mechanism that is presumably independent of the hexosamine pathway (unpublished observations). Additionally, up to 4h incubation of MIN6 cells with tunicamycin is unable to stimulate the phosphorylation of eIF2α (unpublished observations). Another possibility is that PERK activation is mediated through the inhibition of the proteasome, a high consumer of ATP, which in turn may lead to the inhibition of ER-associated protein degradation (ERAD) and the accumulation of unfolded proteins within the ER. In support of this, proteasome inhibition by MG132 stimulates eIF2α phosphorylation [43, 44], although this has been reported to be via the activation of mGCN2 [43]. Alternatively, energy status may directly lead to the inhibition of protein folding [45, 46], as BiP binding to unfolded proteins is dependent on an ADP/ATP cycle in which cellular ATP is consumed [42]. Yet we provide evidence that PERK activation occurs via a mechanism independent of the accumulation of nascent unfolded proteins and processing intermediates in the ER (Fig 5b). On the other hand, it is possible that PERK is activated by the dynamic folding status of an ER resident protein(s), a hypothesis that we currently favour. However, why PERK activation occurs independently of IRE1 activation in glucose deprived β-cells remains unclear.

Glucose causes a rapid increase in the rate of protein synthesis in pancreatic β-cells, however, the mechanism by which glucose does this is poorly understood. The inhibition of eIF2α phosphorylation stimulates a 53% increase in the rate of protein synthesis in glucose deprived cells but is unable to restore protein synthesis to the rates seen in glucose replete cells (Fig. 6aii). Polysome analysis showed that inhibition of eIF2α phosphorylation in glucose deprived cells led to an increase in the amplitude of the polysomal peaks but not in the size of the polysomes. One possible interpretation of these results is that eIF2α dephosphorylation mobilises hitherto untranslated mRNAs onto polysomes.

We and others have shown that incubation of MIN6 cells/islets at low glucose concentration leads to an increase in the expression of proteins associated with the integrated stress response [32, 33], which has been shown in other cell types to be dependent upon eIF2α phosphorylation and important in pre-conditioning cells in becoming resistant to the effects of various cell stresses, including oxidative stress [27, 29, 47]. Therefore, PERK-dependent phosphorylation of eIF2α at low glucose may play a role in protecting pancreatic β-cells against oxidative stress mediated by

physiological rapid increases in glucose concentration.

The activation of PERK through a decrease in the energy status of the cell is unlikely to be a unique feature of the pancreatic β-cell as hypoxia and ischemia/reperfusion, both associated with decreases in intracellular energy status, lead to PERK-dependent phosphorylation of eIF2α in a number of other cell types [48-53].

Figure Legends

Figure 1: PERK in activated by a decrease in glucose concentration. a.) MIN6 cells were mock-infected or infected with AdPERKΔC for 48h. Following infection, the cells were preincubated in KRB in the absence of glucose for 1h. Cells were then treated for a further 1h in KRB containing 0mM glucose, 20mM glucose or 20mM glucose in the presence of 1μM thapsigargin. Proteins were resolved on SDS-PAGE and Western blotted using antisera against phospho eIF2α (Ser51), total PERK or total eIF2α as a loading control. b) MIN6 cells were transfected with control siRNA (Con) or siRNAs directed against PERK (20 and 21). 72h post-microporation, the cells were incubated for 2h in KRB containing 0mM or 20mM glucose. Where indicated, 1μM Thapsigargin was added in the last hour of treatment. Proteins were resolved on SDS-PAGE and Western blotted using antisera against phospho eIF2α (Ser51), total PERK or total eIF2α as a loading control. c) MIN6 cells were mock-infected or infected with AdPERKΔC for 48h. Following infection, the cells were preincubated in KRB in the absence of glucose for 1h.Cells were then treated for a further hour in KRB supplemented with the indicated concentrations of glucose, or as a control 20mM glucose plus 1μM thapsigargin. Cell lysates were separated on SDS-PAGE and Western blotted using antisera against phospho-eIF2α (Ser51) or eIF2α as a loading control.

Figure 2: PERK is activated by mitochondrial inhibitors. MIN6 cells were pre-incubated for 1h in KRB. Cells were then treated for a further hour in KRB at either 0mM or 20mM glucose in the absence or presence of either 10nM rotenone (Rot), 1μM oligomycin (Oli) or 5mM sodium azide (Azi). Treatments were performed in the presence of [^{35}S]-methionine. a) Lysates were separated on SDS-PAGE and Western blotted using antisera against phospho-eIF2α (Ser51), PERK and eIF2α as a loading control. b) Intracellular ATP content determined as described in Materials and Methods and expressed as nmol of ATP per mg of total protein (n=3, ± S.D.).

Figure 3.Decreases in energy status parallel increases in PERK and eIF2α phosphorylation. MIN6 cells were preincubated for 1h in KRB in the absence of glucose. Cells were then treated for a further hour

in the presence of [^{35}S]-methionine at 0mM or 20mM glucose, or 20mM glucose in the presence of the indicated concentrations of oligomycin. a) intracellular ATP content was assessed as described in Materials and Methods and expressed as nmol of ATP per mg of total protein (n=3, ± S.D.). b) and c) Cell lysates were separated on SDS-PAGE and Western blotted using antisera against phospho AMPK (Thr172) , PERK, phospho-eIF2α (Ser51) or total eIF2α as a loading control. d) Incorporation of [^{35}S]-methionine into total protein expressed as percentage of control (KRB 0mM) (n=3, ± S.D.). e) Post infection with AdPERKΔC, MIN6 cells were pre-incubated in KRB for 1h, before treatment for a further hour in KRB in the absence or presence of 20mM glucose, or 20mM glucose and the indicated concentrations of oligomycin. Cell lysates were separated on SDS-PAGE and Western blotted using antisera against phospho-eIF2α (Ser51), total PERK and eIF2α as a loading control.

Figure 4. AMPK activation does not stimulate eIF2α phosphorylation. a) MIN6 cells were pre-incubated for 1h in KRB. Cells were then treated for a further hour in KRB in the absence or presence of 20mM glucose, or 20mM glucose and the indicated concentrations of AICAR. Treatments were performed in the presence of [^{35}S]-methionine. a) Cell lysates were separated on SDS-PAGE and Western blotted using antisera against phospho-eIF2α (Ser51), phospho-AMPK (Thr172) and total eIF2α as a loading control. b) Incorporation of [^{35}S]-methionine into total protein expressed as a percentage of control (KRB 0mM) (n=3, ± S.E.).

Figure 5. PERK is activated by a mechanism independent of IRE1 activation and the accumulation of nascent unfolded proteins. ai.) MIN6 cells were incubated in KRB (0) or KRB supplemented with 20mM glucose (20) for 2h. Where indicated, 1μM thapsigargin was added in the last hour of treatment. lysates were separated by SDS-PAGE and immunoblotted using antibodies against phospho-IRE1α (Ser724) and IRE1α. aii.) RNA was isolated from MIN6 cells grown in complete media (C) and MIN6 cells incubated in KRB (0mM) or KRB supplemented with 0.5mM glucose or 20mM glucose plus or minus 1μM thapsigargin (Thaps) for the times indicated. Spliced and unspliced forms of XBP1 mRNA were amplified by RT-PCR, digested with Pst1 and the fragments separated on an agarose gel. b) MIN6 cells were pulsed for 15min with [^{35}S]-methionine (P) prior to incubation for 1h in KRB in the absence (-) or presence (+) of 0.1mg/ml cycloheximide (Preinc). The cells were then incubated for a further hour in KRB in the continued presence of cycloheximide where indicated (+), at either 0mM or 20mM glucose. bi) Cell lysates were then separated on a 20% SDS-PAGE and labelled proteins visualised by autoradiography. The positions of proinsulin (PI) and insulin (Ins) are indicated. bii) Cell lysates were

separated on SDS-PAGE and Western blotted using antisera against phospho-eIF2α (Ser51) or total eIF2α as a loading control.

Figure 6. The role of eIF2α phosphorylation in glucose stimulated protein synthesis. MIN6 cells were infected with control Ad-Empty virus (Empty) or infected with AdPERKΔC (PERKΔC) or AdGADDΔN (GADDΔN) for 48h. a) Following infection, the cells were incubated for 2h in KRB at 0mM glucose, 20mM glucose or 20mM glucose in the presence of 1μM thapsigargin for the last hour. ai) Proteins were resolved on SDS-PAGE and Western blotted using antisera against phospho eIF2α (Ser51), total PERK or total eIF2α as a loading control. aii) [^{35}S]-methionine incorporation into total protein expressed as a percentage of control (Ad-Empty-KRB/0mM) (n=3, ±Av.D.) *p* values obtained using a 2-tailed T-test. aiii.) [^{35}S]-methionine incorporation into Proinsulin (PI) was also assessed on SDS-PAGE. b) Alternatively, after treatments, cells were lysed and polysome analysis was carried out using 20-50% sucrose gradients. The gradients were fractionated from top (fraction 1) to bottom (fraction 20). Absorbance of the gradients was measured continually at 254nm to give polysome profiles.

References

1 **Rutter, G. A. (2001) Nutrient-secretion coupling in the pancreatic islet beta-cell: recent advances. Mol Aspects Med 22, 247-284**

2 **Permutt, M. A. (1974) Effect of glucose on initiation and elongation rates in isolated rat pancreatic islets. J Biol Chem 249, 2738-2742**

3 **Itoh, N., Sei, T., Nose, K. and Okamoto, H. (1978) Glucose stimulation of the proinsulin synthesis in isolated pancreatic islets without increasing amount of proinsulin mRNA. FEBS Lett 93, 343-347**

4 **Itoh, N. and Okamoto, H. (1980) Translational control of proinsulin synthesis by glucose. Nature 283, 100-102**

5 **Guest, P. C., Rhodes, C. J. and Hutton, J. C. (1989) Regulation of the biosynthesis of insulin-secretory-granule proteins. Co-ordinate translational control is exerted on some, but not all, granule matrix constituents. Biochem J 257, 431-437**

6 **Alarcon, C., Lincoln, B. and Rhodes, C. J. (1993) The biosynthesis of the subtilisin-related proprotein convertase PC3, but no that of the PC2 convertase, is regulated**

by glucose in parallel to proinsulin biosynthesis in rat pancreatic islets. J Biol Chem 268, 4276-4280

7 Skelly, R. H., Schuppin, G. T., Ishihara, H., Oka, Y. and Rhodes, C. J. (1996) Glucose-regulated translational control of proinsulin biosynthesis with that of the proinsulin endopeptidases PC2 and PC3 in the insulin-producing MIN6 cell line. Diabetes 45, 37-43

8 Skelly, R. H., Bollheimer, L. C., Wicksteed, B. L., Corkey, B. E. and Rhodes, C. J. (1998) A distinct difference in the metabolic stimulus-response coupling pathways for regulating proinsulin biosynthesis and insulin secretion that lies at the level of a requirement for fatty acyl moieties. Biochem J 331, 553-561

9 Wang, S. Y. and Rowe, J. W. (1988) Age-related impairment in the short term regulation of insulin biosynthesis by glucose in rat pancreatic islets. Endocrinology 123, 1008-1013

10 Martin, S. K., Carroll, R., Benig, M. and Steiner, D. F. (1994) Regulation by glucose of the biosynthesis of PC2, PC3 and proinsulin in (ob/ob) mouse islets of Langerhans. FEBS Lett 356, 279-282

11 Gomez, E., Powell, M. L., Greenman, I. C. and Herbert, T. P. (2004) Glucose-stimulated Protein Synthesis in Pancreatic β-Cells Parallels an Increase in the Availability of the Translational Ternary Complex (eIF2-GTP.Met-tRNAi) and the Dephosphorylation of eIF2α. J. Biol. Chem. 279, 53937-53946

12 Grimaldi, K. A., Siddle, K. and Hutton, J. C. (1987) Biosynthesis of insulin secretory granule membrane proteins. Control by glucose. Biochem J 245, 567-573

13 Wicksteed, B., Alarcon, C., Briaud, I., Lingohr, M. K. and Rhodes, C. J. (2003) Glucose-induced translational control of proinsulin biosynthesis is proportional to preproinsulin mRNA levels in islet beta-cells but not regulated via a positive feedback of secreted insulin. J Biol Chem 278, 42080-42090

14 Hinnebusch, A. G. (2000) Mechanism and regulation of methionyl-tRNA binding to ribosomes. In Translational Control of Gene Expression. (Sonenberg, N., Hershey,J.W.B. and Mathews,M.B., ed.), pp. pp. 185–243., Cold Spring Harbor Laboratory Press, Cold Spring Harbor, NY.

15 Proud, C. G. (2005) eIF2 and the control of cell physiology. Semin Cell Dev Biol 16, 3-12

16 Welsh, G. I., Miller, C. M., Loughlin, A. J., Price, N. T. and Proud, C. G. (1998) Regulation of eukaryotic initiation factor eIF2B: glycogen synthase kinase-3 phosphorylates a conserved serine which undergoes dephosphorylation in response to insulin. FEBS Lett 421, 125-130

17 Wang, X., Paulin, F. E., Campbell, L. E., Gomez, E., O'Brien, K., Morrice, N. and Proud, C. G. (2001) Eukaryotic initiation factor 2B: identification of multiple phosphorylation sites in the epsilon-subunit and their functions in vivo. Embo J 20, 4349-4359.

18 Kimball, S. R. and Jefferson, L. S. (1995) Allosteric regulation of eukaryotic initiation factor eIF-2B by adenine nucleotides. Biochem Biophys Res Commun 212, 1074-1081

19 Singh, L. P. and Wahba, A. J. (1995) Allosteric activation of rabbit reticulocyte guanine nucleotide exchange factor activity by sugar phosphates and inositol phosphates. Biochem Biophys Res Commun 217, 616-623

20 Price, N. T., Welsh, G. I. and Proud, C. G. (1991) Phosphorylation of only serine-51 in protein synthesis initiation factor-2 is associated with inhibition of peptide-chain initiation in reticulocyte lysates. Biochem Biophys Res Commun 176, 993-999

21 Kimball, S. R., Fabian, J. R., Pavitt, G. D., Hinnebusch, A. G. and Jefferson, L. S. (1998) Regulation of guanine nucleotide exchange through phosphorylation of eukaryotic initiation factor eIF2α. Role of the α- and δ- subunits of eIF2B. J Biol Chem 273, 12841-12845

22 Clemens, M. J. and Elia, A. (1997) The double-stranded RNA-dependent protein kinase PKR: structure and function. J Interferon Cytokine Res 17, 503-524

23 Jagus, R., Joshi, B. and Barber, G. N. (1999) PKR, apoptosis and cancer. Int J Biochem Cell Biol 31, 123-138

24 Sood, R., Porter, A. C., Olsen, D. A., Cavener, D. R. and Wek, R. C. (2000) A mammalian homologue of GCN2 protein kinase important for translational control by phosphorylation of eukaryotic initiation factor-2α. Genetics 154, 787-801.

25 Yang, R., Wek, S. A. and Wek, R. C. (2000) Glucose limitation induces GCN4 translation by activation of Gcn2 protein kinase. Mol Cell Biol 20, 2706-2717.

26 Chen, J. J., Crosby, J. S. and London, I. M. (1994) Regulation of heme-regulated eIF-2 alpha kinase and its expression in erythroid cells. Biochimie 76, 761-769

27 Harding, H. P., Zhang, Y., Bertolotti, A., Zeng, H. and Ron, D. (2000) Perk is essential for translational regulation and cell survival during the unfolded protein response. Mol Cell 5, 897-904.

28 Harding, H. P., Zhang, Y. and Ron, D. (1999) Protein translation and folding are coupled by an endoplasmic-reticulum-resident kinase. Nature 397, 271-274

29 Harding, H. P., Novoa, I., Zhang, Y., Zeng, H., Wek, R., Schapira, M. and Ron, D. (2000) Regulated translation initiation controls stress-induced gene expression in mammalian cells. Mol Cell 6, 1099-1108.

30 Scheuner, D., Song, B., McEwen, E., Liu, C., Laybutt, R., Gillespie, P., Saunders, T., Bonner-Weir, S. and Kaufman, R. J. (2001) Translational control is required for the unfolded protein response and in vivo glucose homeostasis. Mol Cell 7, 1165-1176.

31 Scheuner, D., Mierde, D. V., Song, B., Flamez, D., Creemers, J. W., Tsukamoto, K., Ribick, M., Schuit, F. C. and Kaufman, R. J. (2005) Control of mRNA translation preserves endoplasmic reticulum function in beta cells and maintains glucose homeostasis. Nat Med 11, 757-764

32 Elouil, H., Bensellam, M., Guiot, Y., Vander Mierde, D., Pascal, S. M., Schuit, F. C. and Jonas, J. C. (2007) Acute nutrient regulation of the unfolded protein response and integrated stress response in cultured rat pancreatic islets. Diabetologia 50, 1442-1452

33 Greenman, I. C., Gomez, E., Moore, C. E. and Herbert, T. P. (2007) Distinct glucose-dependent stress responses revealed by translational profiling in pancreatic beta-cells. J Endocrinol 192, 179-187

34 Vander Mierde, D., Scheuner, D., Quintens, R., Patel, R., Song, B., Tsukamoto, K., Beullens, M., Kaufman, R. J., Bollen, M. and Schuit, F. C. (2007) Glucose activates a protein phosphatase-1-mediated signaling pathway to enhance overall translation in pancreatic beta-cells. Endocrinology 148, 609-617

35 Herbert, T. P., Kilhams, G. R., Batty, I. H. and Proud, C. G. (2000) Distinct Signalling Pathways Mediate Insulin and Phorbol Ester-stimulated Eukaryotic Initiation Factor 4F Assembly and Protein Synthesis in HEK 293 Cells. J Biol Chem 275, 11249-11256

36 Calfon, M., Zeng, H., Urano, F., Till, J. H., Hubbard, S. R., Harding, H. P., Clark, S. G. and Ron, D. (2002) IRE1 couples endoplasmic reticulum load to secretory capacity by processing the XBP-1 mRNA. Nature 415, 92-96

37 Marciniak, S. J., Yun, C. Y., Oyadomari, S., Novoa, I., Zhang, Y., Jungreis, R., Nagata, K., Harding, H. P. and Ron, D. (2004) CHOP induces death by promoting protein synthesis and oxidation in the stressed endoplasmic reticulum. Genes Dev 18, 3066-3077

38 Cardozo, A. K., Ortis, F., Storling, J., Feng, Y. M., Rasschaert, J., Tonnesen, M., Van Eylen, F., Mandrup-Poulsen, T., Herchuelz, A. and Eizirik, D. L. (2005) Cytokines downregulate the sarcoendoplasmic reticulum pump Ca2+ ATPase 2b and deplete endoplasmic reticulum Ca2+, leading to induction of endoplasmic reticulum stress in pancreatic beta-cells. Diabetes 54, 452-461

39 Hardie, D. G. (2003) Minireview: the AMP-activated protein kinase cascade: the key sensor of cellular energy status. Endocrinology 144, 5179-5183

40 Bertolotti, A., Zhang, Y., Hendershot, L. M., Harding, H. P. and Ron, D. (2000) Dynamic interaction of BiP and ER stress transducers in the unfolded- protein response. Nat Cell Biol 2, 326-332.

41 Ma, K., Vattem, K. M. and Wek, R. C. (2002) Dimerization and release of molecular chaperone inhibition facilitate activation of eukaryotic initiation factor-2 kinase in response to endoplasmic reticulum stress. J Biol Chem 277, 18728-18735

42 Schroder, M. and Kaufman, R. J. (2005) ER stress and the unfolded protein response. Mutat Res 569, 29-63

43 Jiang, H. Y. and Wek, R. C. (2005) Phosphorylation of the alpha-subunit of the eukaryotic initiation factor-2 (eIF2alpha) reduces protein synthesis and enhances apoptosis in response to proteasome inhibition. J Biol Chem 280, 14189-14202

44 Cowan, J. L. and Morley, S. J. (2004) The proteasome inhibitor, MG132, promotes the reprogramming of translation in C2C12 myoblasts and facilitates the association of hsp25 with the eIF4F complex. Eur J Biochem 271, 3596-3611

45 Tagliavacca, L., Wang, Q. and Kaufman, R. J. (2000) ATP-dependent dissociation of non-disulfide-linked aggregates of coagulation factor VIII is a rate-limiting step for secretion. Biochemistry 39, 1973-1981

46 Mirazimi, A. and Svensson, L. (2000) ATP is required for correct folding and disulfide bond formation of rotavirus VP7. J Virol 74, 8048-8052

47 Harding, H. P., Zhang, Y., Zeng, H., Novoa, I., Lu, P. D., Calfon, M., Sadri, N., Yun, C., Popko, B., Paules, R., Stojdl, D. F., Bell, J. C., Hettmann, T., Leiden, J. M. and Ron, D. (2003) An integrated stress response regulates amino acid metabolism and resistance to oxidative stress. Mol Cell 11, 619-633

48 Montie, H. L., Kayali, F., Haezebrouck, A. J., Rossi, N. F. and Degracia, D. J. (2005) Renal ischemia and reperfusion activates the eIF 2α kinase PERK. Biochim Biophys Acta 1741, 314-324

49 Owen, C. R., Kumar, R., Zhang, P., McGrath, B. C., Cavener, D. R. and Krause, G. S. (2005) PERK is responsible for the increased phosphorylation of eIF2α and the severe inhibition of protein synthesis after transient global brain ischemia. J Neurochem 94, 1235-1242

50 Emadali, A., Nguyen, D. T., Rochon, C., Tzimas, G. N., Metrakos, P. P. and Chevet, E. (2005) Distinct endoplasmic reticulum stress responses are triggered during human liver transplantation. J Pathol 207, 111-118

51 Bi, M., Naczki, C., Koritzinsky, M., Fels, D., Blais, J., Hu, N., Harding, H., Novoa, I., Varia, M., Raleigh, J., Scheuner, D., Kaufman, R. J., Bell, J., Ron, D., Wouters, B. G. and Koumenis, C. (2005) ER stress-regulated translation increases tolerance to extreme hypoxia and promotes tumor growth. Embo J 24, 3470-3481

52 Blais, J. D., Filipenko, V., Bi, M., Harding, H. P., Ron, D., Koumenis, C., Wouters, B. G. and Bell, J. C. (2004) Activating transcription factor 4 is translationally regulated by hypoxic stress. Mol Cell Biol 24, 7469-7482

53 Koumenis, C., Naczki, C., Koritzinsky, M., Rastani, S., Diehl, A., Sonenberg, N., Koromilas, A. and Wouters, B. G. (2002) Regulation of protein synthesis by hypoxia

via activation of the endoplasmic reticulum kinase PERK and phosphorylation of the translation initiation factor eIF2α. Mol Cell Biol 22, 7405-7416

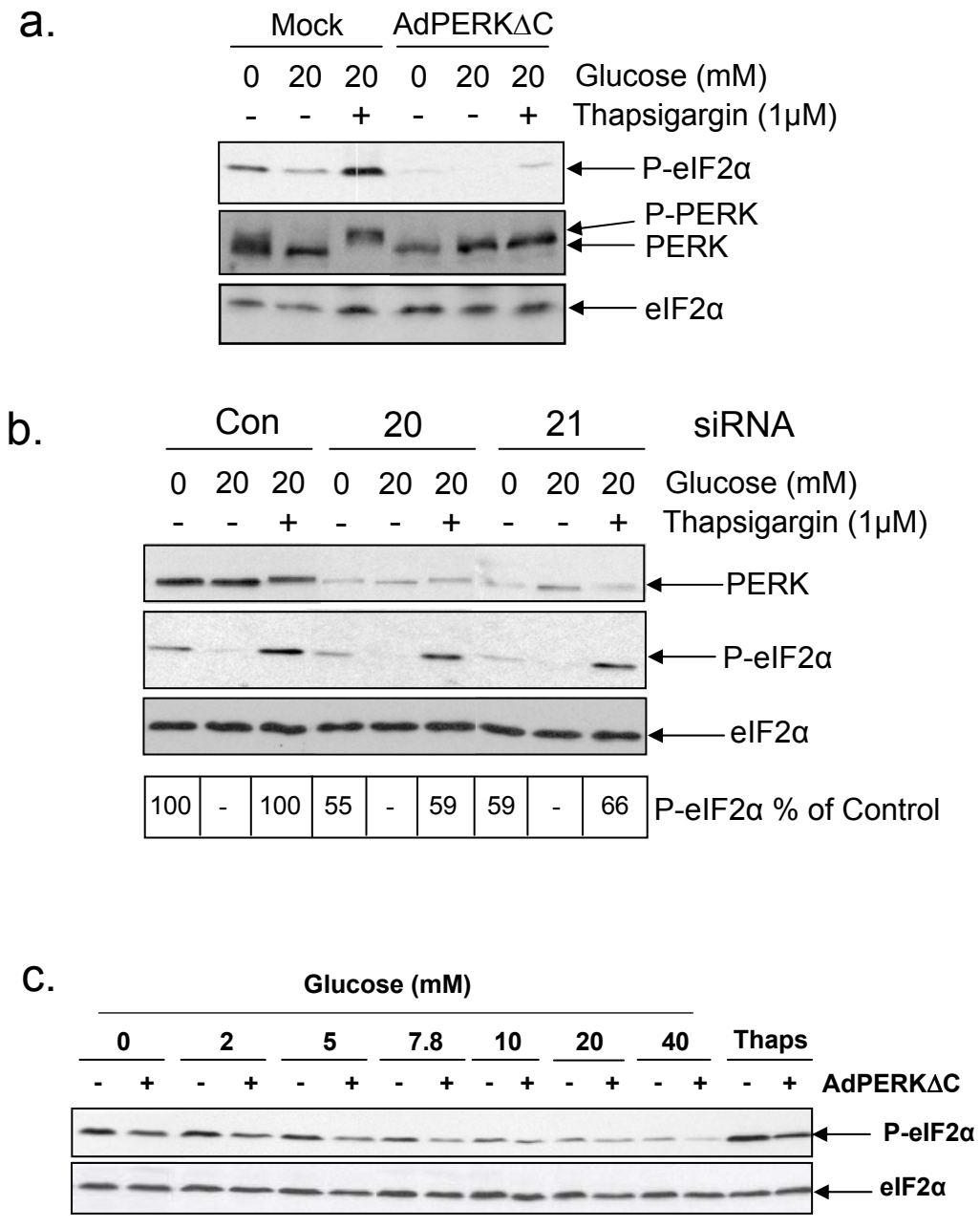
a.
Mock
AdPERKΔC
0 20 20 0 20 20 Glucose (mM)
- - + - - + Thapsigargin (1μM)
P-eIF2α
P-PERK
PERK
eIF2α
b.
Con
20
21
siRNA
0 20 20 0 20 20 0 20 20 Glucose (mM)
- - + - - + - - + Thapsigargin (1μM)
PERK
P-eIF2α
eIF2α
100 - 100 55 - 59 59 - 66 P-eIF2α % of Control
c.
Glucose (mM)
0 2 5 7.8 10 20 40 Thaps
- + - + - + - + - + - + - + - + AdPERKΔC
P-eIF2α
eIF2α

Figure 1

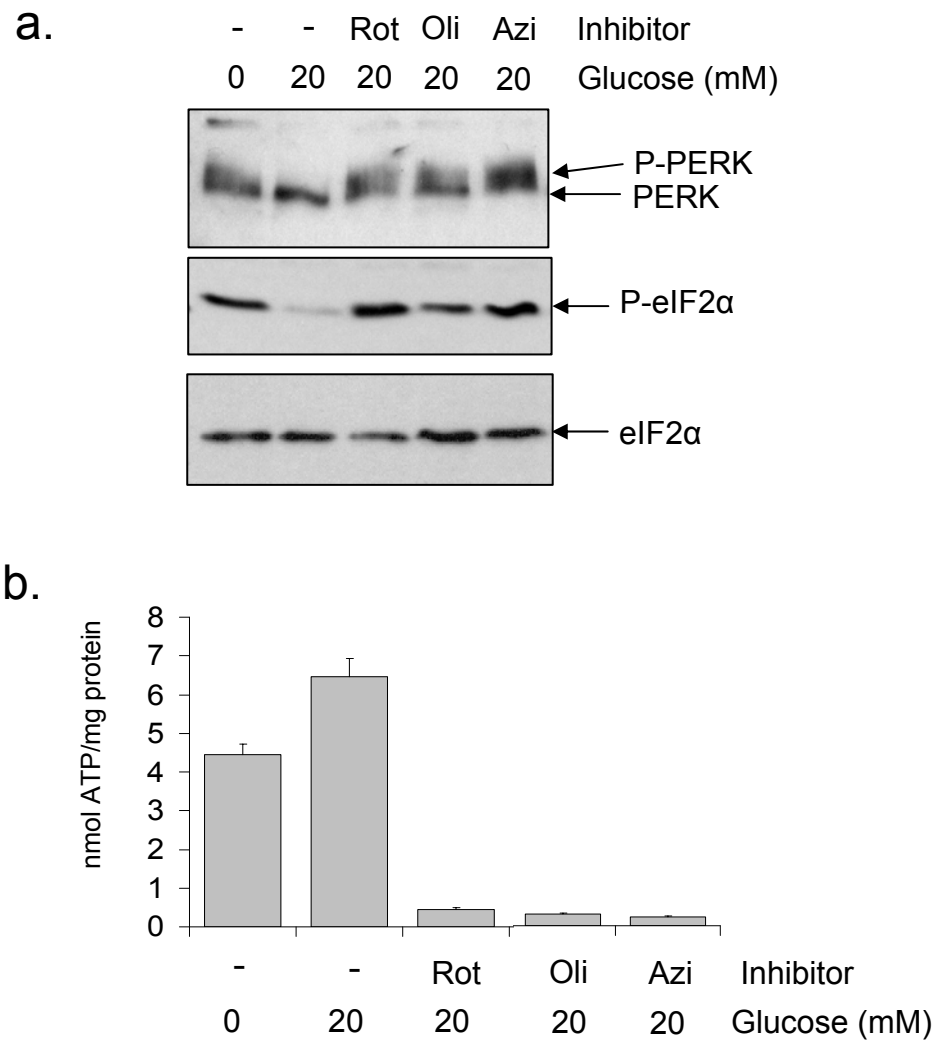
a.
- - Rot Oli Azi Inhibitor
0 20 20 20 20 Glucose (mM)
P-PERK
PERK
P-eIF2α
eIF2α
b.
nmol ATP/mg protein
8
7
6
5
4
3
2
1
0
- - Rot Oli Azi Inhibitor
0 20 20 20 20 Glucose (mM)

Figure 2

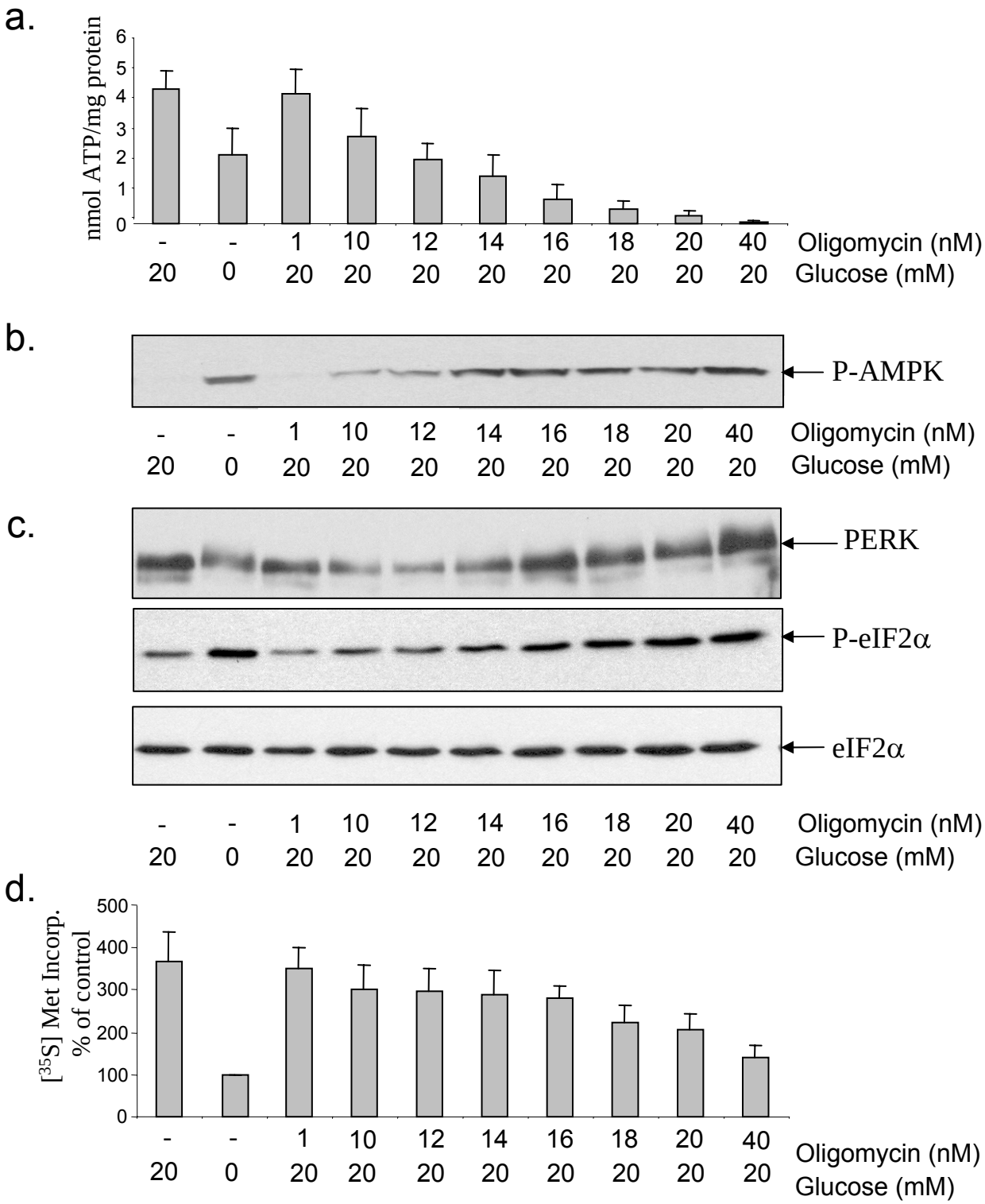
a.
nmol ATP/mg protein
0
1
2
3
4
5
6
- - 1 10 12 14 16 18 20 40 Oligomycin (nM)
20 0 20 20 20 20 20 20 20 20 Glucose (mM)
b.
P-AMPK
- - 1 10 12 14 16 18 20 40 Oligomycin (nM)
20 0 20 20 20 20 20 20 20 20 Glucose (mM)
c.
PERK
P-eIF2α
eIF2α
- - 1 10 12 14 16 18 20 40 Oligomycin (nM)
20 0 20 20 20 20 20 20 20 20 Glucose (mM)
d.
[35S] Met Incorp.
% of control
0
100
200
300
400
500
- - 1 10 12 14 16 18 20 40 Oligomycin (nM)
20 0 20 20 20 20 20 20 20 20 Glucose (mM)
e.
10nM 20nM 40nM [Oligomycin]
0 0 20 20 20 20 20 20 20 20 Glucose (mM)
- + - + - + - + - + AdPERKΔC
P-PERK
PERK
P-eIF2α
eIF2α

Figure 3

a.

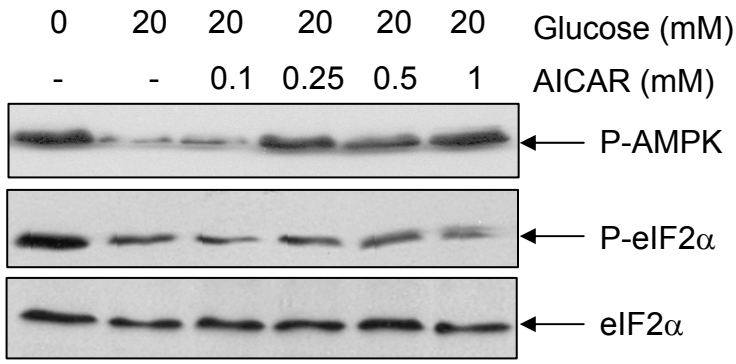
0 20 20 20 20 20 Glucose (mM)
- - 0.1 0.25 0.5 1 AICAR (mM)
P-AMPK
P-eIF2α
eIF2α

b.

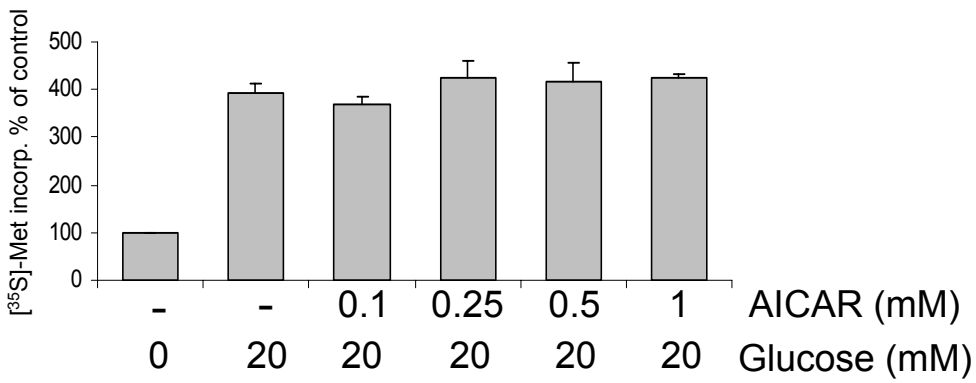
[35S]-Met incorp. % of control
500
400
300
200
100
0
- - 0.1 0.25 0.5 1 AICAR (mM)
0 20 20 20 20 20 Glucose (mM)

Figure 4

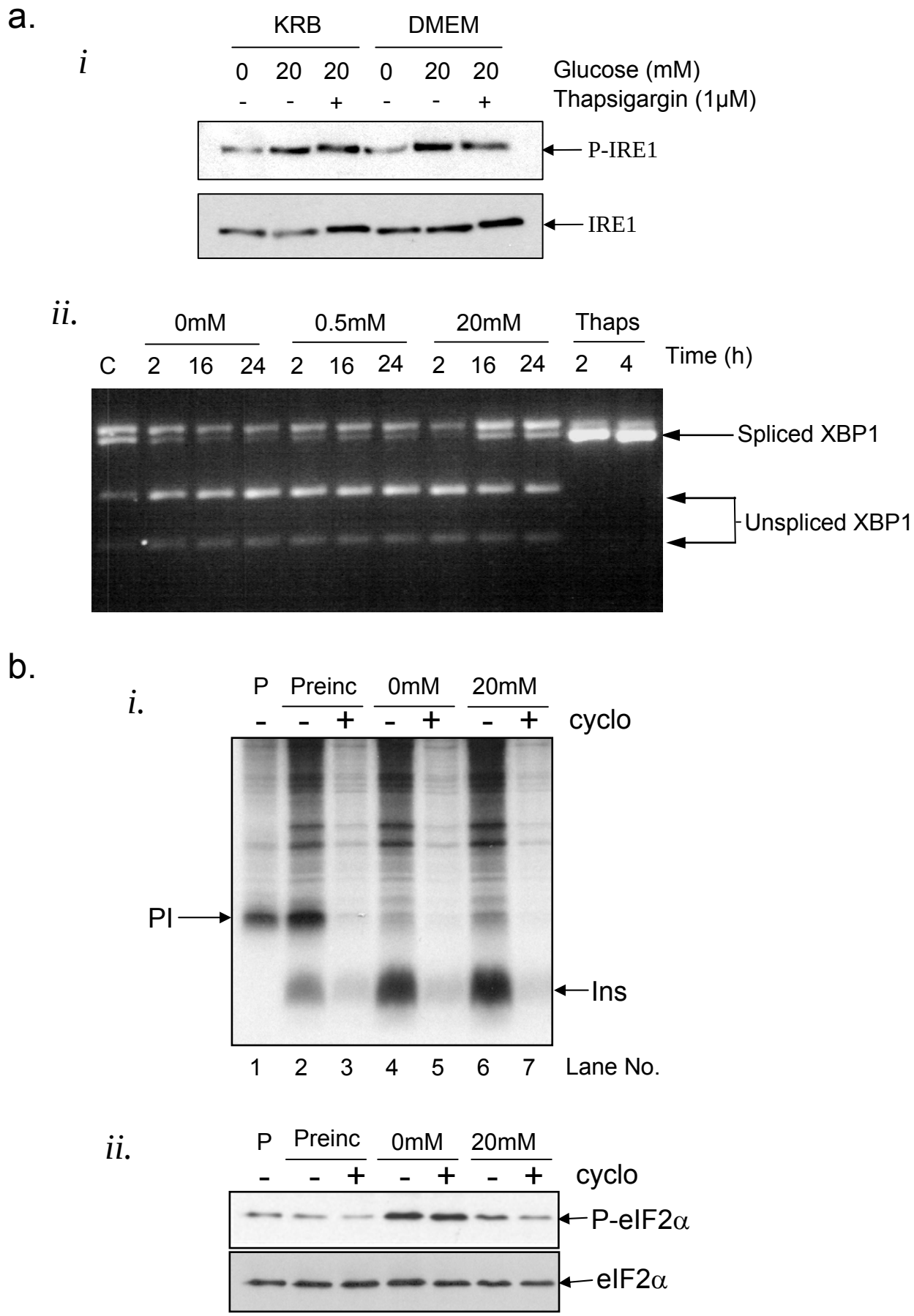
a.
i
KRB
DMEM
0 20 20 0 20 20
Glucose (mM)
- - + - - +
Thapsigargin (1μM)
P-IRE1
IRE1
ii.
0mM
0.5mM
20mM
Thaps
C 2 16 24 2 16 24 2 16 24 2 4
Time (h)
Spliced XBP1
Unspliced XBP1
b.
i.
P
Preinc
0mM
20mM
- - + - + - +
cyclo
PI
Ins
1 2 3 4 5 6 7
Lane No.
ii.
P
Preinc
0mM
20mM
- - + - + - +
cyclo
P-eIF2α
eIF2α

Figure 5

a.

i.

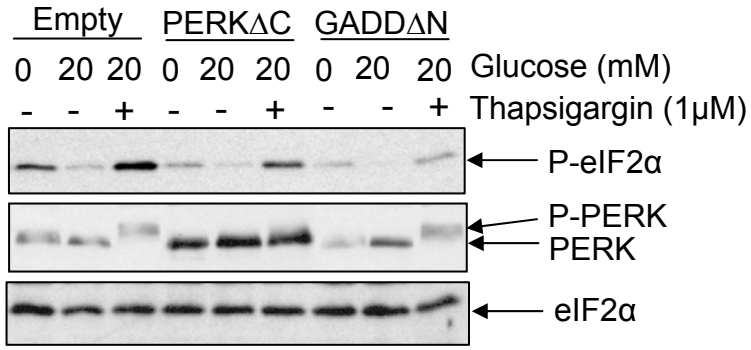

ii.

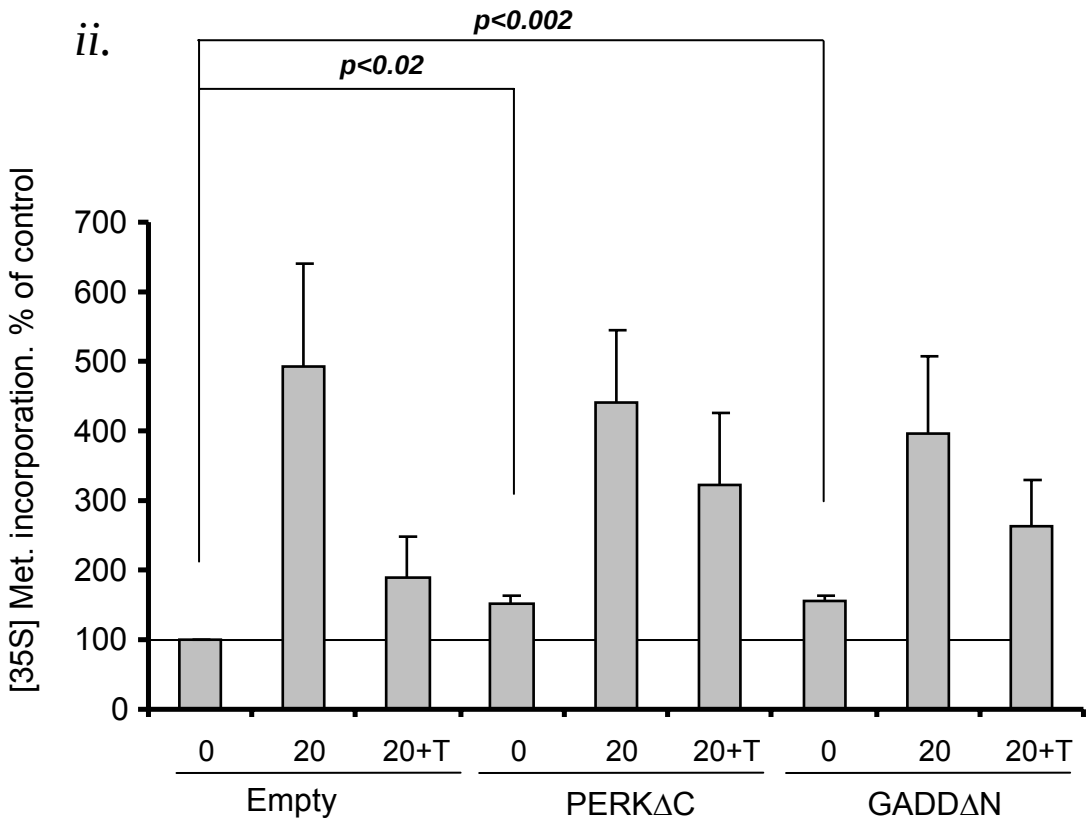

iii.

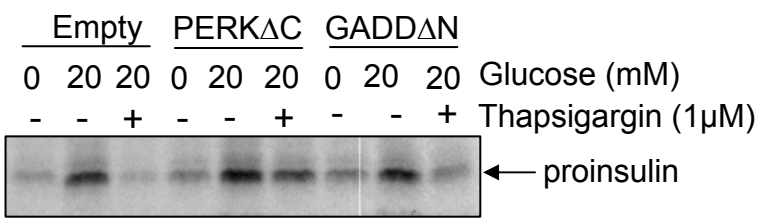

Figure 6

b.

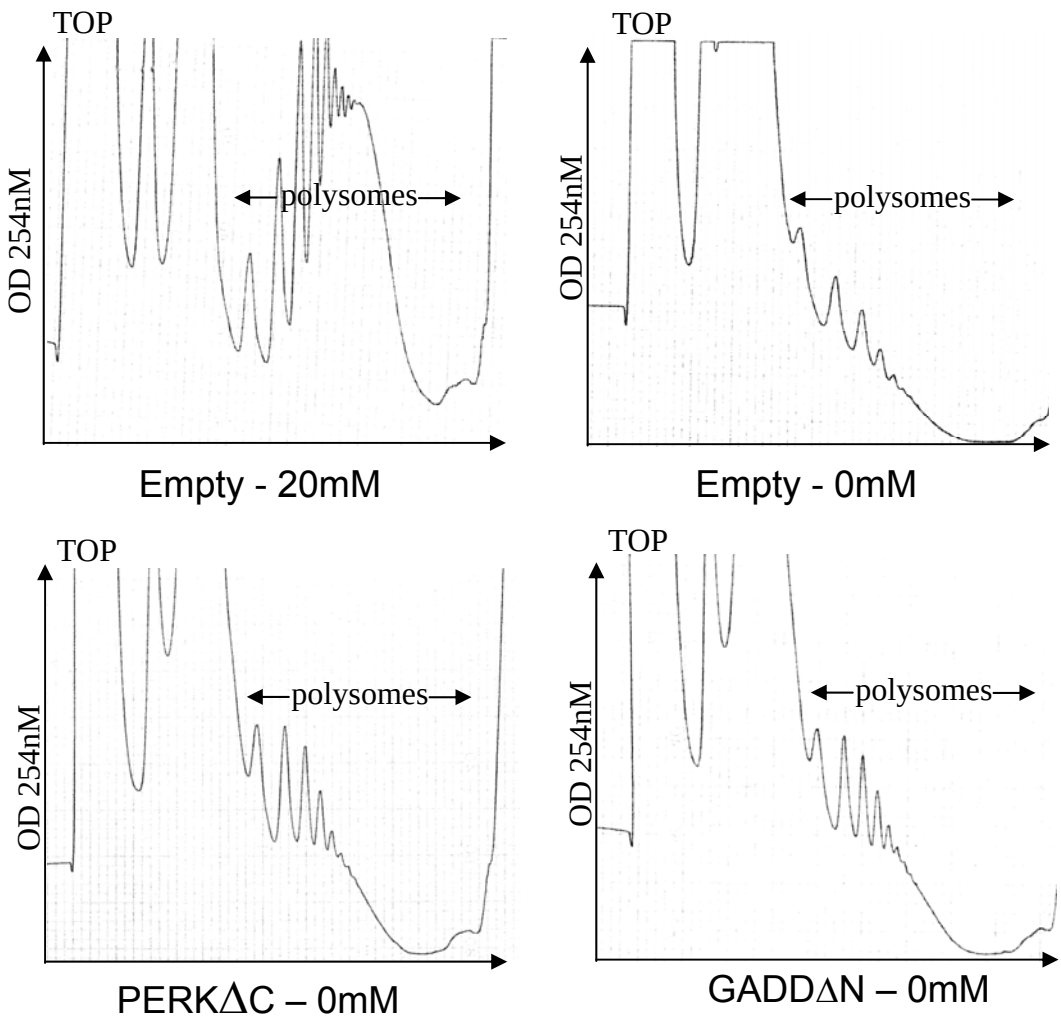

Figure 6 continued